JACS
JOURNAL OF THE AMERICAN CHEMICAL SOCIETY

COMMUNICATION

pubs.acs.org/JACS

A Highly Thermally Stable Ferroelectric Metal−Organic Framework and Its Thin Film with Substrate Surface Nature Dependent Morphology

Chen Pan,[†,‡] Jiangpu Nan,[†] Xueliang Dong,[†] Xiao-Ming Ren,[*,†,‡] and Wanqin Jin[*,†]

[†]State Key Laboratory of Materials-Oriented Chemical Engineering and [‡]College of Science, Nanjing University of Technology, Nanjing 210009, P. R. China

Supporting Information

ABSTRACT: A highly thermally stable, polar MOF built from the rigid ligand benzene-1,4-dicarboxylate and the main-group metal ion Sr^{2+} shows ferroelectricity. With the ultimate goal of making components for use in devices, the fabrication of MOF thin films on Al_2O_3, $SrAl_2O_4$, and Al foil substrates using the in situ solvothermal method was explored. The mechanism of macroscopic polarization reversals in the ferroelectric MOF under an ac electric field and the dependence of the morphology of the MOF thin film on the nature of the substrate surface are discussed.

Recently developed metal−organic frameworks (MOFs) or porous coordination polymers are breakthrough materials characterized by tunable pores permeating regular molecular scaffolds.[1] These hybrid solids couple the variety of potential ligands from coordination chemistry with the topological diversity of solid-state chemistry and have found many applications in gas adsorption[2] and storage,[3] molecular separation,[4] and catalysis.[5] Additionally, there are increasing numbers of studies on MOFs with switchable properties that depend on the interaction between the framework and guest molecules.[6] For example, guest-dependent spin-crossover function was imparted to MOFs by incorporation of electronically switching Fe^{2+} ions into the porous molecular framework,[7] proton conductivity in hybrid materials was obtained via the rational design of proton carriers into MOFs,[1a,8] an electro-optic material with reorientation of molecules controlled by an applied electric field was achieved using a MOF crystal as a carrier for rotary polar groups,[9] and new electronic and photoactive microporous materials were created by utilizing conducting dithiolene-based MOFs.[10]

MOFs also provide a new promising platform for creating polar crystalline materials that possess technologically important physical properties relevant to fields from optics to electronics.[11] Comparing of the reports to date on the adsorption of small molecules, even if studies on polar-functionalized MOFs (such as ferroelectric MOFs) have lagged behind, there still are exciting examples: an intriguing ferroelectricity was observed in the MOF $[Mn_3(HCOO)_6](C_2H_5OH)$,[12] where the ethanol molecules are loosely bound guests in the pores and their ordering results in net polarization, and a paraelectric−ferroelectric transition was triggered by freezing disordered NH_4^+ countercations by incorporating the H-bond donor NH_4^+ cation into the negatively charged metal formate framework of $[Zn(HCOO)_3]^-$.[13]

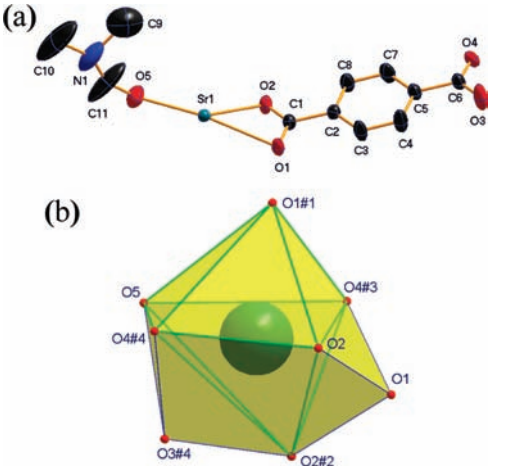

Figure 1. (a) Asymmetric unit of **1** with thermal ellipsoids at the 50% probability level. (b) Coordination octahedron of the Sr^{2+} ion in **1**. Atoms marked with # are at the following symmetry positions: #1 = $-x+y, 1-x, -^1/_3+z$; #2 = $1-y, 1+x-y, ^1/_3+z$; #3 = $-1+x, y, z$; #4 = $1-x+y, 2-x, -^1/_3+z$.

Apart from their use as bulk materials, MOFs are also potential candidates for thin-film applications.[14] Pioneering works on MOF films or membranes in regard to film or membrane growth and applications in molecular separation and luminescence functionalities have already been reported,[15] but exploration of the preparation of thin films and their dielectric and ferroelectric properties is quite rare and remains an important challenge. In this communication, we present the ferroelectric and dielectric properties of a highly thermally stable MOF, $[Sr(DMF)(\mu\text{-BDC})]_\infty$ (**1**) (DMF = *N*,*N*-dimethylformamide; BDC^{2-} = benzene-1,4-dicarboxylate), and our results showing the facile growth of thin films of **1** on a variety of functional substrates, such as the surfaces of $SrAl_2O_4$, porous Al_2O_3, and Al foil.

Colorless needle-shaped single crystals of **1** were obtained through a solvothermal process at 100 °C [see the Supporting Information (SI)]; the reaction temperature strongly influenced the resultant purity, and the pure phase was obtained only when the reaction temperature was between 90 and 110 °C. The crystals of **1** belong to the trigonal space group $P3_1$ at room temperature, with an asymmetric unit consisting of one Sr^{2+} ion, one BDC^{2-} ligand, and one DMF molecule (Figure 1a). The Sr^{2+}

Received: April 6, 2011
Published: July 21, 2011

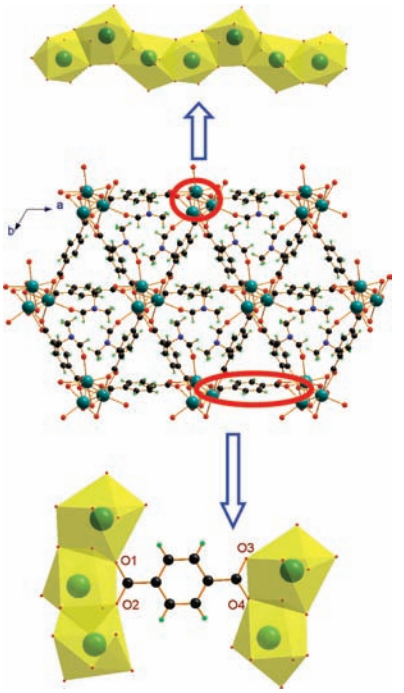

Figure 2. Packing diagram of **1** projected along the *c* axis, showing the inorganic chains of bicapped octahedra and the connectivity between them.

ion is coordinated by eight oxygen atoms from five BDC^{2-} ligands and one DMF molecule, which form a distorted bicapped coordination octahedron. The DMF molecule acts as a monodentate ligand, and the two carboxylate groups of a BDC^{2-} ligand show different binding modes with Sr^{2+} ions: one of them (containing the O1 atom) is bound to three Sr^{2+} ions in an η^2:η^2-bridging mode, while another (containing the O3 atom) is connected to two Sr^{2+} ions in an η^1:η^2-bridging mode. As shown in Figure 1b, the Sr−O bond lengths range from 2.483(4) to 2.766(3) Å in the bicapped octahedron, with Sr1−O5 (from the DMF molecule) having the shortest bond distance; the cis and trans O−Sr−O bond angles within the coordination octahedron are in the ranges 63.42(9)−116.20(10)° and 147.84(14)−162.58(11)°, respectively, which heavily deviate from the corresponding ideal angles of 90 and 180°. The O−Sr−O bond angles between the capping and neighboring O atoms are in the range 48.09(9)−77.72(9)° for O1 versus 48.70(10)−83.94(16)° for O3#4 (symmetry code #4 = $1 - x + y$, $2 - x$, $-{}^1/_3 + z$); the geometric parameters in the coordination sphere are similar to those reported in the literature.[16] Neighboring bicapped coordination octahedra are connected into a zigzag inorganic chain via face-sharing along the crystallographic *c* direction, and adjacent inorganic chains are linked into three-dimensional framework by the BDC^{2-} ligands, which adopt a μ_5,η^1:η^2:η^2:η^2-bridging mode (Figure 2). This MOF exhibits two types of triangular channels; the smaller channels are empty, and the larger ones are filled with DMF molecules that are bound directly to the Sr^{2+} ions.

MOF **1** shows high thermal stability. Thermogravimetric analysis (TGA) under a nitrogen flow (air atmosphere) revealed that the removal of the coordinated DMF molecules occurs between 265 and 350 °C (230 and 350 °C) and that collapse of the framework begins at ∼500 °C (>400 °C). It is well-known that DMF decomposes above its boiling point (151 °C), and it is worthy of mention that the thermal stability of the DMF molecules in **1** is much increased as a result of the coordination interaction with the Sr^{2+} ions. Since **1** crystallizes in a noncentrosymmetric space group ($P3_1$) belonging to the polar point groups C_3, its second-order nonlinear optical behavior and ferroelectric and dielectric properties were investigated. The study of a powdered sample, in which the crystallite size was not optimized, indicated that the second-harmonic generation efficiency of **1** is ∼0.4 times that of urea.

A single crystal of **1** with an approximate size of 0.2 mm × 0.2 mm × 0.5 mm was selected for the dielectric hysteresis loop measurement. Two electrodes were made of Au wire with a diameter of 80 μm and attached by Ag-conducting glue on two opposite surfaces of the crystal that were approximately parallel to the (001) crystal face. The measurements were performed on a ferroelectric tester (Radient Technology) under various alternating current (ac) electric fields at room temperature, and the typical polarization versus applied electric field (P−E) curve is displayed in Figure 3a. The estimated values of the characteristic ferroelectric parameters under an applied electric field of 1.98 kV cm^{-1} were the following: saturation spontaneous polarization, $P_s \approx 0.83$ μC cm^{-2}; remanent polarization, $P_r \approx 0.48$ μC cm^{-2}; and coercive field, $E_c \approx 0.81$ kV cm^{-1}.

A ferroelectric hysteresis indicates that the macroscopic polarization in the ferroelectric material is being reversed or switched. This macroscopic polarization reversal implies local, microscopic polarization reversal, which includes electronic, atomic, and ionic displacement polarization reversals as well as permanent dipole reversal under an ac electric field. From a structural viewpoint, the polarization reversal could be achieved via DMF displacement occurring along the Sr−O(DMF) bond direction within a coordination sphere, since there exists a weak ion−dipole interaction between the Sr^{2+} ion and the DMF O atom and the DMF molecules swing along the *c* direction, as schematically illustrated in Figure 3b and confirmed by the crystal data at 403 and 243 K.

The dielectric property of **1** was further investigated, and plots of the dielectric constant (ε') versus temperature and the dielectric loss [tan(δ)] versus temperature at different frequencies as well as the frequency dependence of ε' and tan(δ) at different temperatures are displayed in Figure 3c,d and Figure S11 in the SI. These figures show the following features: (1) **1** has an invariant ε' (∼4.6) as well as a constant tan(δ) (∼5.0 × 10^{-3}) in the low-temperature regime below 270 K; (2) both the dielectric constant and dielectric loss rapidly increase when the temperature rises above 300 K, and no peak maximum appears in the plots of ε' versus T below 433 K; (3) the increases in the dielectric constant and dielectric loss with temperature depend strongly on the frequency of the ac electric filed, which is obvious when the frequency is below 10^3 Hz. The dielectric relaxation originating from electronic transitions or molecular vibrations has frequencies above 10^{12} Hz, and the dielectric relaxation arising from dipole motion or ionic polarization occurs in the frequency range 10^2−10^{10} Hz. Therefore, the relaxation appearing in 1−10^7 Hz could be attributed to slow dipole, ionic, or molecular motion in the crystals of **1**.

In order to understand the observed dielectric properties and the possible molecular motion under an ac electric field, variable-temperature single-crystal X-ray crystallography and differential scanning calorimetry (DSC) were conducted for **1**. Generally speaking, the crystal structures at 243 and 403 K are very similar to that at 293 K (Tables S1 and S2 and Figures S6−S8). All of the Sr−O bond distances in the bicapped octahedron increased

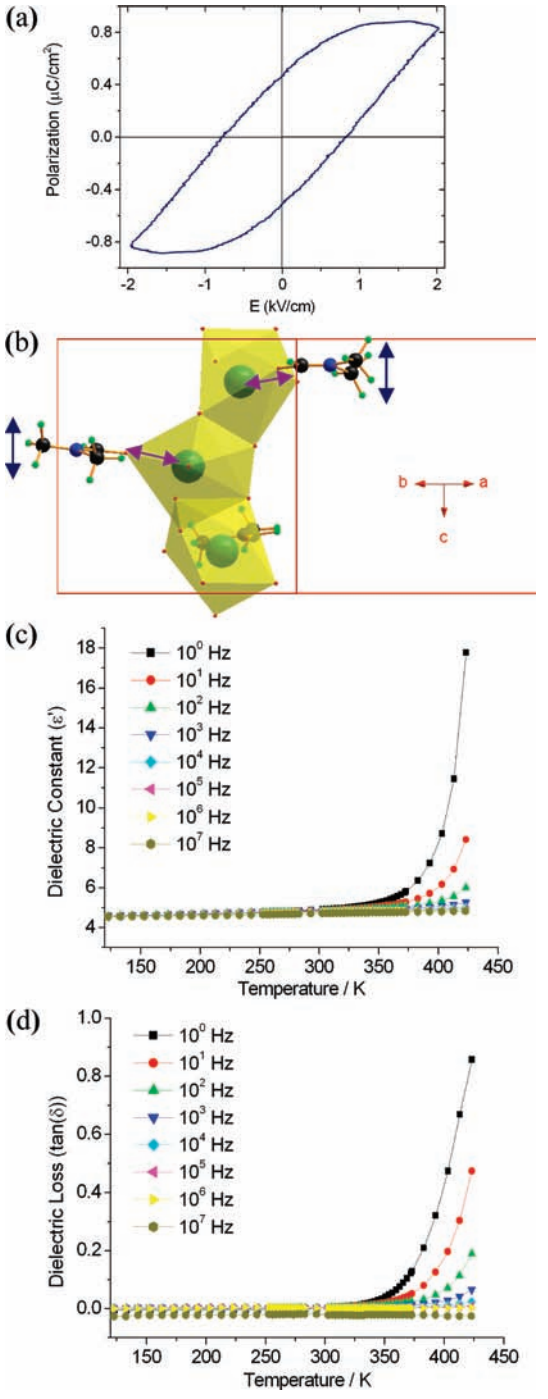

Figure 3. (a) Hysteresis loop in the $P-E$ plot for **1** at room temperature. (b) Schematic illustration of the polarization reversal under an ac electric field via motions of DMF molecules in the directions shown by the arrows. (c, d) Temperature dependence of (c) the dielectric constant ε' and (d) the dielectric loss $\varepsilon''/\varepsilon'$ at various frequencies ($1-10^7$ Hz), .

slightly as the temperature rose from 293 to 403 K. However, it was found that the Sr−O bond distances decreased upon cooling from 293 to 243 K, except for Sr1−O5 (where O5 is from the coordinated DMF molecule) (Table S2). On the other hand, as shown in Tables S3 and S4, the isotropic temperature factors U_{iso} and the anisotropic temperature factor U_{33} for the non-hydrogen atoms in DMF are larger than those for the other non-hydrogen atoms in **1**; the anisotropic temperature factor U_{33} for all of the non-hydrogen atoms increased with the temperature rise from 243 to 403 K. The thermal motion of the DMF molecules becomes so strong that it exhibits structural disorder with two sites at 403 K, and the disorder-to-order transformation of the DMF molecules is reflected in the DSC plot (Figure S5c). A broad endothermal peak was observed with an onset temperature of ~361 K and $\Delta H \approx 4.79$ kJ mol^{-1}; the transition entropy was estimated as 13.3 J mol^{-1} K^{-1}, which is obviously larger than the entropy change for a disorder−order transition with two disordered sites. As remarked above, it is possible that DMF moves along the Sr−O(DMF) bond direction within a coordination sphere and swings along the c direction under an applied ac electric field, and the increase in both the dielectric constant and dielectric loss above 300 K is probably concerned with the motion of the DMF molecules.

Although some progress has been made in the creation of MOF materials with ferroelectricity[12,13] or a dielectric phase transition,[17] for such kinds of MOFs, their paraelectric−ferroelectric transition or dielectric transition originates from the strong interactions between the framework and the guest molecules or counterions. To the best of our knowledge, our report is the first example of a MOF showing ferroelectricity arising directly from the motion of the ions or molecules in the framework.

Ferroelectric materials have demonstrated remarkable utility in microwave devices (such as dielectric resonators and filters for microwave communication systems) in the form of thin films. In recent years, much of the attention in this field has been focused on the studies of traditional inorganic ferroelectric films, and reports on ferroelectric thin films of inorganic−organic hybrids are rare.[18] We have been focusing our attention on the exploration of ferroelectric thin films of MOFs grown on some typical substrates (porous Al_2O_3, $SrAl_2O_4$, and Al foil, which could have metal oxide surfaces with a high affinity for carboxylic groups). In this work, thin films of **1** were grown by the in situ solvothermal method; the selected substrates were mounted perpendicular to a Teflon-lined autoclave bottom and immersed completely in a DMF solution containing $Sr(NO_3)_2$ and H_2BDC to allow growth of the MOF thin film at 100 °C for 24 h; the cleaned and dried thin-film samples were characterized by scanning electron microscopy (SEM) and X-ray diffraction techniques.

Figure 4 shows the surface morphologies and cross-section microstructures of thin films of **1** on Al_2O_3, $SrAl_2O_4$, and Al foil. Continuous and highly integrated MOF thin films were grown on the Al_2O_3 and $SrAl_2O_4$ substrates, while a continuous grass-like MOF thin film covered the Al foil uniformly with an approximate thickness of 50 μm, with the nanocrystalline grass leaves showing a similar size. The XRD diffraction patterns of thin films covered on three different substrates are in good agreement with the simulated X-ray diffraction pattern from single-crystal data for **1** (Figures S12−S14), indicating that the prepared MOF thin films contain pure phase of **1**. It is noteworthy that the morphologies of the MOF thin films grown on different substrates are distinct from each other and thus obviously depend on the surface chemistry and structure of the substrate. The continuous thin films were obtained only after the surface of the substrate was polished; dense coatings of **1** were achieved on the substrates with a surface consisting of grains, as can be seen in the cross sections in the Al_2O_3 and $SrAl_2O_4$ SEM images (Figure 4b,d), and the oriented MOF thin film was only grown on the Al foil, which has a continuous surface.

In summary, we have reported a polar MOF constructed from the main-group metal ion Sr^{2+} and the rigid BDC^{2-} ligand. This

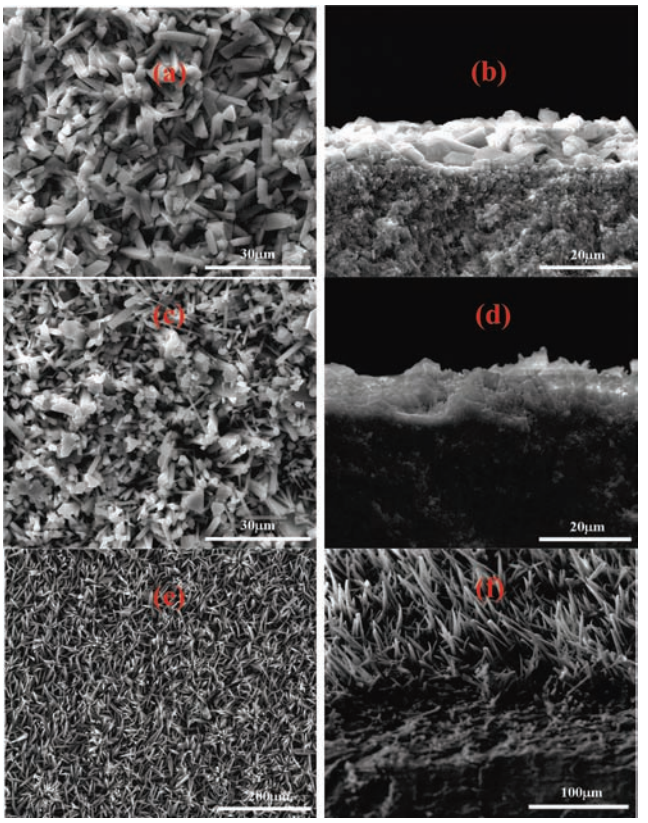

Figure 4. (a) SEM images of thin films of **1**: (a, c, e) top views and (b, d, f) cross sections of films grown on (a,b) Al_2O_3, (c,d) $SrAl_2O_4$, and (e,f) Al foil.

MOF compound shows ferroelectricity. The macroscopic polarization reversals probably arise from the motions of the coordinated DMF molecules under an applied ac field. With the ultimate goal of making components for use in devices, we have explored the fabrication of MOF thin films on different substrates by the in situ solvothermal method. Our study has provided evidence that the growth of polycrystalline thin films of phase-pure **1** directly from the mixed solution of H_2BDC and $Sr(NO_3)_2$ on suitably pretreated substrates is facile, that the morphology of the MOF thin film obviously depends on the surface chemistry and structure of the substrate, and that an oriented MOF thin film can be grown on the surface Al foil. Work on measuring the ferroelectric and dielectric properties for the films of **1** is in progress.

■ ASSOCIATED CONTENT

Supporting Information. Crystallographic data; PXRD, TGA, and DSC profiles; and temperature and ac-frequency dependence of dielectric constants and losses. This material is available free of charge via the Internet at http://pubs.acs.org.

■ AUTHOR INFORMATION

Corresponding Author
xmren@njut.edu.cn; wqjin@njut.edu.cn

■ ACKNOWLEDGMENT

We thank the National Natural Science Foundation of China (Grant 20871068) and the National Basic Research Program of China (2009CB623406) for financial support.

■ REFERENCES

(1) (a) Hurd, J. A.; Vaidhyanathan, R.; Thangadurai, V.; Ratcliffe, C. I.; Moudrakovski, I. L.; Shimizu, G. K. H. *Nat. Chem.* **2009**, *1*, 705. (b) Kitagawa, S.; Matsuda, R. *Coord. Chem. Rev.* **2007**, *251*, 2490. (c) Yaghi, O. M.; O'Keeffe, M.; Ockwig, N. W.; Chae, H. K.; Eddaoudi, M.; Kim, J. *Nature* **2003**, *423*, 705.

(2) (a) Eddaoudi, M.; Kim, J.; Rosi, N.; Vodak, D.; Wachter, J.; O'Keeffe, M.; Yaghi, O. M. *Science* **2002**, *295*, 469. (b) Kitagawa, S.; Kitaura, R.; Noro, S. I. *Angew. Chem., Int. Ed.* **2004**, *43*, 2334. (c) Férey, G. *Chem. Soc. Rev.* **2008**, *37*, 191.

(3) (a) Dincă, M.; Dailly, A.; Liu, Y.; Brown, C. M.; Neumann, D. A.; Long, J. R. *J. Am. Chem. Soc.* **2006**, *128*, 16876. (b) Zhao, X. B.; Xiao, B.; Fletcher, A. J.; Thomas, K. M.; Bradshaw, D.; Rosseinsky, M. J. *Science* **2004**, *306*, 1012.

(4) Pan, L.; Olson, D. H.; Ciemnolonski, L. R.; Heddy, R.; Li, J. *Angew. Chem., Int. Ed.* **2006**, *45*, 632.

(5) (a) Dang, D. B.; Wu, P. Y.; He, C.; Xie, Z.; Duan, C. Y. *J. Am. Chem. Soc.* **2010**, *132*, 14321. (b) Banerjee, M.; Das, S.; Yoon, M.; Choi, H. J.; Hyun, M. H.; Park, S. M.; Seo, G.; Kim, K. *J. Am. Chem. Soc.* **2009**, *131*, 7524. (c) Park, K. H.; Jang, K.; Son, S. U.; Sweigart, D. A. *J. Am. Chem. Soc.* **2006**, *128*, 8740.

(6) Yanai, N.; Kaneko, W.; Yoneda, K.; Ohba, M.; Kitagawa, S. *J. Am. Chem. Soc.* **2007**, *129*, 3496.

(7) Halder, G. J.; Kepert, C. J.; Moubaraki, B.; Murray, K. S.; Cashion, J. D. *Science* **2002**, *298*, 1762.

(8) Sadakiyo, M.; Yamada, T.; Kitagawa, H. *J. Am. Chem. Soc.* **2009**, *131*, 9906.

(9) Winston, E. B; Lowell, P. J.; Vacek, J.; Chocholoušová, J.; Michl, J.; Price, J. C. *Phys. Chem. Chem. Phys.* **2008**, *10*, 5188.

(10) Kobayashi, Y.; Jacobs, B.; Allendorf, M. D.; Long, J. R. *Chem. Mater.* **2010**, *22*, 4120.

(11) (a) Hu, P. H.; Chen, J.; Deng, J. X.; Xing, X. R. *J. Am. Chem. Soc.* **2010**, *132*, 1925. (b) Horiuchi, S.; Tokunaga, Y.; Giovannetti, G.; Picozzi, S.; Itoh, H.; Shimano, R.; Kumai, R.; Tokura, Y. *Nature* **2010**, *463*, 789. (c) Sun, C. F.; Hu, C. L.; Xu, X.; Ling, J. B.; Hu, T.; Kong, F.; Long, X. F.; Mao, J. G. *J. Am. Chem. Soc.* **2009**, *131*, 9486. (d) Akutagawa, T.; Koshinaka, H.; Sato, D.; Takeda, S.; Noro, S.-I.; Takahashi, H.; Kumai, R.; Tokura, Y.; Nakamura, T. *Nat. Mater.* **2009**, *8*, 342. (e) Guloy, A. M.; Tang, Z. J.; Miranda, P. B.; Srdanov, V. I. *Adv. Mater.* **2001**, *13*, 833.

(12) Cui, H. B.; Wang, Z. M.; Takahashi, K.; Okano, Y.; Kobayashi, H.; Kobayashi, A. *J. Am. Chem. Soc.* **2006**, *128*, 15074.

(13) Xu, G. C.; Ma, X. M.; Zhang, L.; Wang, Z. M.; Gao, S. *J. Am. Chem. Soc.* **2010**, *132*, 9588.

(14) Shekhah, O.; Liu, J.; Fischer, R. A.; Wöll, C. *Chem. Soc. Rev.* **2011**, *40*, 1081.

(15) (a) Hermes, S.; Schröder, F.; Chelmowski, R.; Wöll, C.; Fischer, R. A. *J. Am. Chem. Soc.* **2005**, *127*, 13744. (b) Shekhah, O.; Wang, H.; Kowarik, S.; Schreiber, F.; Paulus, M.; Tolan, M.; Sternemann, C.; Evers, F.; Zacher, D.; Fischer, R. A.; Wöll, C. *J. Am. Chem. Soc.* **2007**, *129*, 15118. (c) Biemmi, E.; Scherb, C.; Bein, T. *J. Am. Chem. Soc.* **2007**, *129*, 8054. (d) Ranjan, R.; Tsapatsis, M. *Chem. Mater.* **2009**, *21*, 4920. (e) Bux, H.; Liang, F. Y.; Li, Y. S.; Cravillon, J.; Wiebcke, M.; Caro, J. *J. Am. Chem. Soc.* **2009**, *131*, 16000. (f) Guo, H. L.; Zhu, Y. Z.; Qiu, S. L.; Lercher, J. A.; Zhang, H. J. *Adv. Mater.* **2010**, *22*, 4190. (g) Venna, S. R.; Carreon, M. A. *J. Am. Chem. Soc.* **2010**, *132*, 76. (h) Makiura, R.; Motoyama, S.; Umemura, Y.; Yamanaka, H.; Sakata, O.; Kitagawa, H. *Nat. Mater.* **2010**, *9*, 565. (i) Liu, B.; Ma, M. Y.; Zacher, D.; Bétard, A.; Yusenko, K.; Metzler-Nolte, N.; Wöll, C.; Fischer, R. A. *J. Am. Chem. Soc.* **2011**, *133*, 1734.

(16) Williams, C. A.; Blake, A. J.; Wilson, C.; Hubberstey, P.; Schröder, M. *Cryst. Growth Des.* **2008**, *8*, 911.

(17) Zhang, W.; Cai, Y.; Xiong, R. G.; Yoshikawa, H.; Awaga, K. *Angew. Chem., Int. Ed.* **2010**, *49*, 6758.

(18) Li, X. L.; Chen, K.; Liu, Y.; Wang, Z. X.; Wang, T. W.; Zuo, J. L.; Li, Y. Z.; Wang, Y.; Zhu, J. S.; Liu, J. M.; Song, Y.; You, X. Z. *Angew. Chem., Int. Ed.* **2007**, *46*, 6820.